Journal of Hazardous Materials 344 (2018) 408–416

Contents lists available at ScienceDirect

Journal of Hazardous Materials

journal homepage: www.elsevier.com/locate/jhazmat

Research Paper

Photocatalytic reusable membranes for the effective degradation of tartrazine with a solar photoreactor

L. Aoudjit[a,b,1], P.M. Martins[c,d,*,1], F. Madjene[a], D.Y. Petrovykh[e], S. Lanceros-Mendez[c,f,g,*]

[a] Unité de Développement des équipements Solaires, UDES/Centre de Développement des Energies Renouvelables, CDER, Bou Ismail, 42415, W. Tipaza, Algeria
[b] Laboratoire de Chimie du Gaz Naturel, Faculté de Chimie, BP 32, 16111, El Alia, U.S.T.H.B., Bab Ezzouar, Algeria
[c] Centre/Departament of Physics, University of Minho, Campus de Gualtar, 4710-057 Braga, Portugal
[d] CEB – Centre of Biological Engineering, University of Minho, 4710-057 Braga, Portugal
[e] International Iberian Nanotechnology Laboratory, Avenida Mestre José Veiga, 4715-330 Braga, Portugal
[f] BCMaterials, Parque Científico y Tecnológico de Bizkaia, 48160 Derio, Spain
[g] IKERBASQUE, Basque Foundation for Science, 48013 Bilbao, Spain

HIGHLIGHTS

- TiO_2 nanoparticles were immobilized on PVDF-TrFE for photocatalytic degradation of tartrazine.
- A solar photoreactor was used for the photocatalytic experiments.
- The dependence of tartrazine concentration on photocatalysis efficiency was addressed.
- The light intensity and the reusability of the of the TiO_2/PVDF-TrFE membranes was tested.

GRAPHICAL ABSTRACT

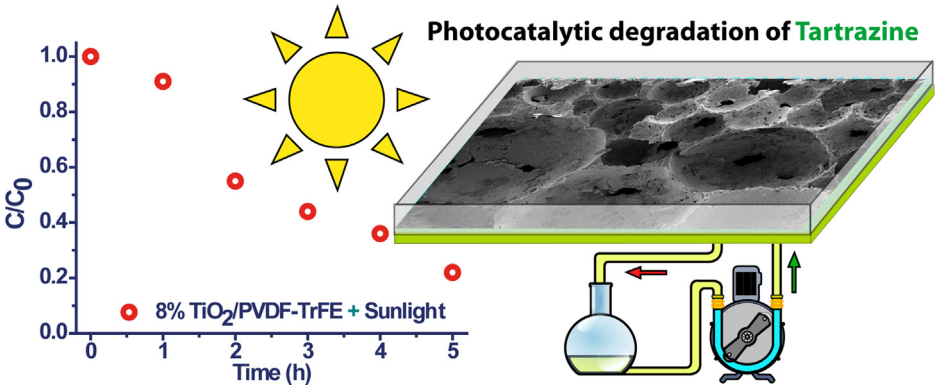

ARTICLE INFO

Article history:
Received 1 June 2017
Received in revised form 9 October 2017
Accepted 25 October 2017

Keywords:
Azo-dye
Micropollutants
Photoreactor
PVDF-TrFE
Solar photocatalysis

ABSTRACT

Recalcitrant dyes present in effluents constitute a major environmental concern due to their hazardous properties that may cause deleterious effects on aquatic organisms. Tartrazine is a widely-used dye, and it is known to be resistant to biological and chemical degradation processes and by its carcinogenic and mutagenic nature. This study presents the use of TiO_2 (P25) nanoparticles immobilized into a poly(vinylidenefluoride–trifluoroethylene) (P(VDF–TrFE)) membrane to assess the photocatalytic degradation of this dye in a solar photoreactor. The nanocomposite morphological properties were analyzed, confirming an interconnected porous microstructure and the homogeneous distribution of the TiO_2 nanoparticles within the membrane pores. It is shown that the nanocomposite with 8 wt% TiO_2 exhibits a remarkable sunlight photocatalytic activity over five hours, with 78% of the pollutant being degraded. It was also demonstrated that the degradation follows pseudo-first-order kinetics model at low initial tartrazine concentration. Finally, the effective reusability of the produced nanocomposite was also assessed.

* Corresponding authors at: Centre/Departament of Physics, University of Minho, Campus de Gualtar, 4710-057 Braga, Portugal
E-mail addresses: pamartins@fisica.uminho.pt, pedrmartins@gmail.com (P.M. Martins), senentxu.lanceros@bcmaterials.net (S. Lanceros-Mendez).
[1] These authors contributed equally to this work.

https://doi.org/10.1016/j.jhazmat.2017.10.053
0304-3894/

1. Introduction

Water pollution caused by organic chemicals from textile, paper, plastic, leather, food, and mineral processing industries is a growing problem [1,2], mainly caused by the presence of synthetic dyes in effluents. Estimates show that approximately 10–15% of dyes used in the industry will end up in wastewaters after the manufacturing process [3,4]. Most of these dyes possess complex and stable molecular structures, making them resistant to conventional biological and chemical degradation processes [5,6]. The presence of these dyes in effluents compromises water properties, such as color, pH, sunlight penetration, and chemical oxygen demand, and important ecological impacts as most of these dyes are carcinogenic and genotoxic – associated with oxidative stress [7,8]. Among these dyes, tartrazine (C.I. Acid Yellow 23, AY23) was selected as a model pollutant for the present work. Tartrazine is an azoic dye widely used in the textile, cosmetics, pharmaceutical and food industry [9,10]. In the last decades, many works have reported about tartrazine hazards, identifying its potentially deleterious effects, such as food allergies, mutagenic, carcinogenic and phototoxicity [11–15].

In this context, the development of low-cost and efficient advanced water treatment technologies are urgently needed. There has been significant research on applying photocatalysis for water treatment due to their efficient degradation of organic compounds [16,17]. Photocatalytic reactions allow for complete degradation of organic pollutants into small and harmless species, without using chemicals, thus avoiding sludge production and disposal. Titanium dioxide (TiO_2), a well-known semiconductor, has been applied in air purification, solar energy conversion, and wastewater treatment due to its high photocatalytic activity, low cost, low photo erosion, non-toxicity, and excellent chemical and thermal stability under illumination [18]. In wastewater treatment processes, TiO_2 nanoparticles are used as a slurry system due to the large surface area of the catalysts, which allows high photocatalytic efficiency [19]. Nevertheless, the filtration to separate and recycle the TiO_2 nanoparticles suspended in the treated water significantly increases the running cost and produces collateral pollution. This problem has become a limiting factor in the practical application of photocatalytic slurry systems. To prevent secondary pollution and to allow the reusability of photocatalytic materials, numerous works have been devoted to TiO_2 nanoparticle immobilization into substrates, including glass, zeolites, ceramic particles and polymers, among others [16,20–23]. These materials can be produced by techniques such as sol-gel, electrochemical anodizing, chemical deposition, photo-assisted deposition, solvent casting, grafting, dip coating, electrospinning have been used [20,21,24–27].

Further, together with photocatalytic treatments, membrane processes have also been increasingly applied to treat waste effluents from industry. Membrane separation processes have shown to be competitive with other separation processes regarding energy costs, material recovery, environmental friendliness, and for being simple to integrate into processes for selective removal of impurities [28]. However, this technique just concentrates pollutants, not destroying them. It can be argued that the coupling of a photocatalytic reaction with a membrane separation process could take advantage of the synergy of both technologies. This combination can result in a robust system, with the membrane having the dual task of supporting the photocatalyst as well as acting as a selective barrier for the species to be degraded [2,29]. Membrane separation may be combined with a photocatalysis process in what is called a photocatalytic membrane reactor. In such reactor, the catalysts could be immobilized on the membrane surface or suspended in water [30]. However, most of the works reported concerning photocatalysis use TiO_2 suspended in water.

Many of the most used membranes are based on polymeric materials, mostly for being mechanically stable, chemically inert, inexpensive and easily accessible [31]. The first application of a polymer as a TiO_2 substrate for photocatalytic applications dates back to 1995, where TiO_2 particles were immobilized into a polythene film [32]. In the next years, many other polymers such as poly(vinylidenefluoride), polystyrene, polyethylene glycol and polyamide12, among others, were tested [21,33,34]. Poly(vinylidenefluoride–trifluoroethylene) P(VDF–TrFE) allows the production of membranes with controlled porosity and pore size [35–37]. Its favorable physicochemical properties are suited for photocatalytic application as it shows excellent UV resistance [38], which is paramount to materials continuously exposed to sunlight. Furthermore, it possesses a chemical, mechanical and thermal resistance, related to the stable C–F bonds of the polymer chain [39]. Additionally, this nanocomposite has displayed a remarkable photocatalytic activity in the degradation of methylene blue [37,40].

The principal goal of this work is to demonstrate the suitability and reusability of photocatalytic TiO_2 nanoparticles immobilized on a P(VDF–TrFE) porous membrane in the degradation of tartrazine in a solar photoreactor. Several studies have reported about tartrazine photocatalytic degradation [41–44]. However, few of them focus on the solar radiation and using immobilized catalysts.

2. Experimental

Poly(vinylidene fluoride-trifluoroethylene), (P(VDFTrFE)) 70/30 was purchased to Solvay (Belgium). Titanium dioxide (TiO_2) nanoparticles (P25-Aeroxide), with a surface area ranging from 35 to 65 m^2/g (manufacturer datasheet), were acquired to Evonik Industries AG. Tartrazine (M = 534.36 g/mol) also known as Yellow 23 (Fig. 1a), with the chemical formula $C_{16}H_9N_4Na_3O_9S_2$ and a maximum absorption at the wavelength of 427 nm (Fig. 1b) was purchased to ACROS organics (USA).

2.1. Production of TiO_2/PVDF-TrFE nanocomposite membranes

The poly(vinylidene difluoride)-co-trifluoroethylene (P(VDF-TrFE)) membranes containing titanium dioxide P25 were prepared by solvent casting according to [37]. This filler concentration was selected based on previously reported works [37] to reduce nanoparticles aggregates, detachment from the substrate and preserve the required polymer mechanical properties. Briefly, as represented in Fig. 2, 0.86 g (8 wt.%) of TiO_2 nanoparticles was added to 90 ml of N, N-dimethylformamide (DMF, Merck) and placed in an ultrasound bath for four hours to achieve a good dispersion of the nanoparticles. Then, 10 g of P(VDF-TrFE) was added to the solution, reaching a concentration of 10 wt.% polymer, and kept under magnetic stirring until complete dissolution. Finally, the solution was placed in a glass support to allow solvent evaporation, at room temperature.

After complete evaporation of the solvent, a membrane with the same dimensions of the photoreactor tank surface (38 cm length × 12 cm wide cm) was precisely cut out.

2.2. Characterization of TiO_2/PVDF-TrFE nanocomposite membranes

The microstructure of the produced nanocomposite membranes was evaluated by scanning electron microscopy (SEM). The samples were coated during 30 s with a thin gold layer and analyzed with a Quanta 650 SEM (FEI). Energy dispersive X-ray spectroscopy (EDX) was assessed with an INCA 350 spectrometer (Oxford Instruments).

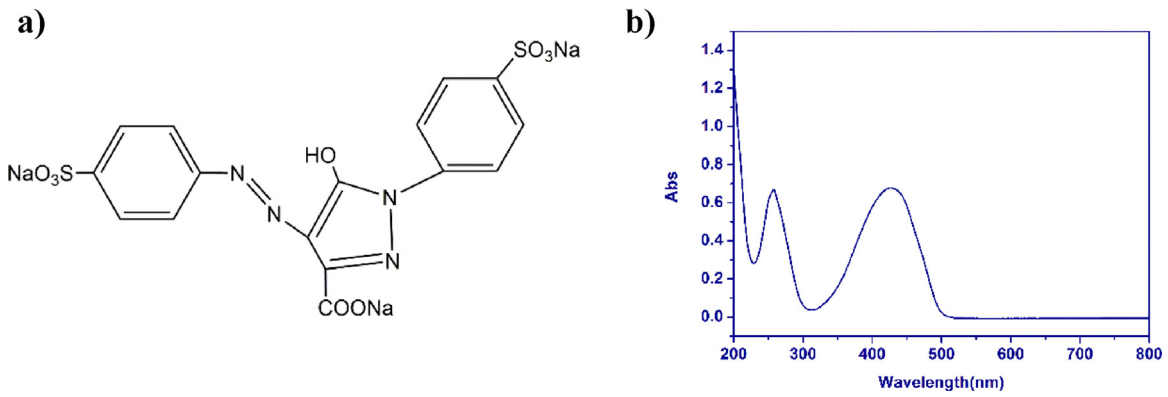

Fig. 1. Tartrazine chemical structure (a) and its UV–vis absorption spectrum in aqueous solution (b).

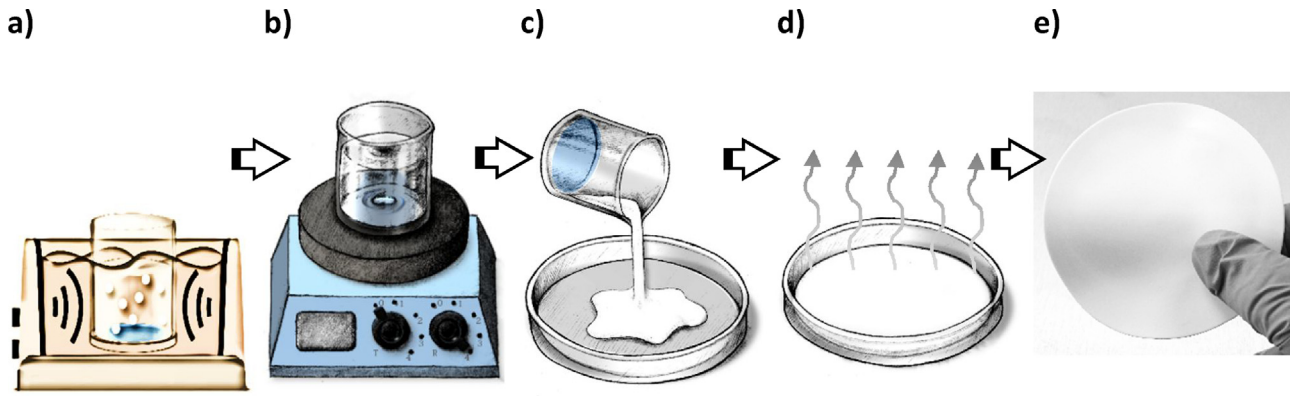

Fig. 2. Schematic representation of the production of the 8% TiO_2/PVDF-TrFE nanocomposite membranes by solvent casting; a) ultrasonic bath of DMF and TiO_2 nanoparticles; b) magnetic stirring of DMF, TiO_2 nanoparticles, and the added PVDF-TrFE; c) pouring the solution on a glass support; d) solvent evaporation at room temperature; e) membrane after complete evaporation of the solvent.

2.3. Photocatalytic degradation of tartrazine

The photocatalytic degradation of tartrazine was carried out in a solar photoreactor located in northern Algeria (latitude 36°.39′; longitude 2°.42′ at sea level), from August to September, using natural solar irradiation. The intensity of solar UV radiation was measured with a Pyranometer CMP 11 (Kipp & Zonen) with a spectral range between 285 and 2800 nm. All the assays performed in this study presented sunlight intensities profiles similar the one shown in the supplementary material (Figure A1).

The reactor was developed at the Solar Equipment Development Unit (UDES) in Algeria. The effective volume of the photoreactor is 1 l (38 cm length × 12 cm wide × 8.5 cm high). The photoreactor tank was fabricated from Pyrex glass, where the produced TiO_2/PVDF-TrFE nanocomposite membrane was placed at the bottom (Fig. 3). The flow rate used for tartrazine solution recirculation was 28 ml s^{-1}; allowing to cover the entire surface of the nanocomposite membrane with the tartrazine solution. The photoreactor was completely covered with a glass to avoid evaporation during the photocatalytic experiments.

For the photocatalytic assays, one liter of tartrazine solution was added to the photoreactor tank containing the 8 wt% TiO_2/P(VDF-TrFE) porous membrane and illuminated with solar light for five hours. The pH of the solution was not adjusted (initial pH ≈ 6.2 and final pH ≈ 4.3), and the temperature was not controlled, varying from 25 to 36 °C. These conditions were selected to evaluate the potential applicability of the system. Tartrazine solutions of 10, 20, and 30 mg/l were prepared to study the effect of initial concentrations on the photocatalytic degradation. A 5 ml sample was withdrawn at one-hour intervals. The influence of flow rate was investigated using a flow rate of 28 ml s^{-1} and 9.8 ml s^{-1} under the same experimental conditions (C_0 = 10 mg l^{-1} under UV for five hours).

To assess the reusability of the produced 8 wt% TiO_2/P(VDF-TrFE) nanocomposite, after the first use the membrane and the photoreactor were washed with distilled water under continuous flow and dried at ambient conditions. Afterwards, a new tartrazine solution (same concentration – 10 mg l^{-1}) was added, and the same procedure was adopted.

Different UV intensities were used in the photocatalytic process; it was used a UV lamp from Phillips (PL-L 24W/10/4P) – with a maximum wavelength peak at 365 nm and an intensity of ≈ 6 mW/cm^2. The lamp was used to irradiate the photoreactor (15 cm distance) with the nanocomposite and the tartrazine solution (10 mg l^{-1}), for five hours. The results were compared with the sunlight photocatalytic degradation.

All the withdrawn samples were analyzed with a UV–visible spectrophotometer (Shimadzu-1800), and the peak at 427 nm was used to monitor tartrazine absorbance over irradiation time. The percentage of degradation was estimated using the following equation (Eq. 1) [45].

$$Degradation\,(\%) = \frac{C_0 - C_t}{C_0} \times 100 \quad (1)$$

where C_o is the initial dye concentration and C_t is the dye concentration after a certain reaction time t (min).

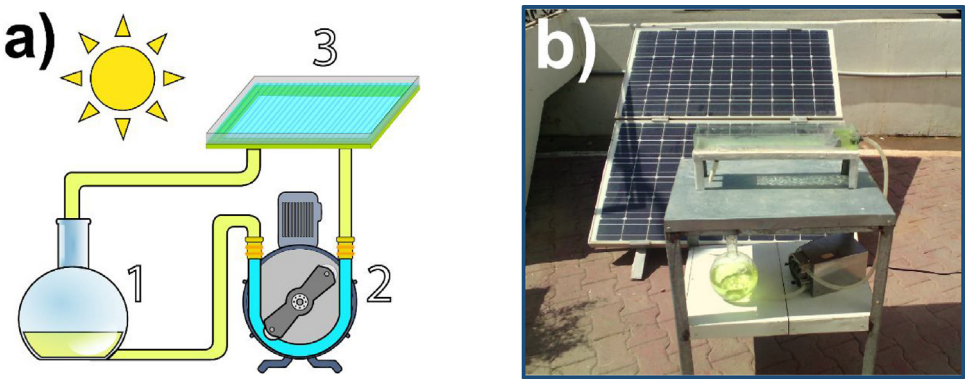

Fig. 3. Schematic representation of the solar photoreactor: *1*- tartrazine solution flask; *2*- peristaltic pump; 3–photoreactor tank with the 8% TiO_2/PVDF-TrFE photocatalytic membrane (a); picture of the photoreactor during the photocatalytic degradation of tartrazine under sunlight irradiation (b).

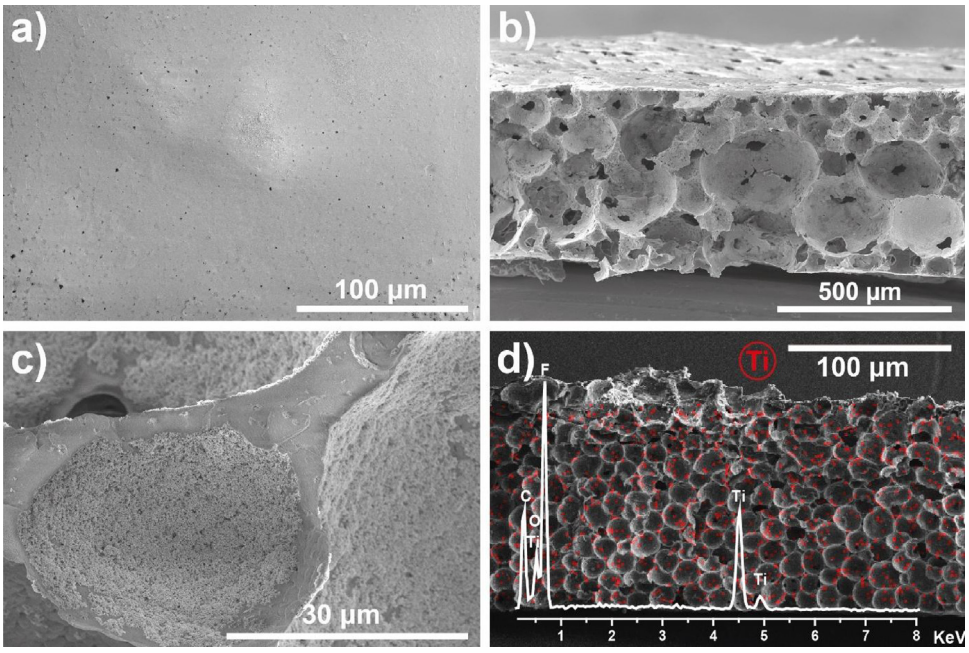

Fig. 4. SEM images of 8 wt% TiO2/P(VDF–TrFE) membranes: Surface (a); cross section (b, c); SEM-EDX mapping image of the presence and distribution of titanium (Ti – red) in the PVDF-TrFE matrix with inset of the EDX spectra with elemental identification (C,F,O, and Ti). (For interpretation of the references to colour in this figure legend, the reader is referred to the web version of this article.)

3. Results and discussion

3.1. TiO_2/PVDF-TrFE nanocomposite membranes characterization

The TiO_2 nanoparticles were immobilized into P(VDF–TrFE) membranes produced by solvent evaporation at room temperature, as previously reported in [37,46]. SEM surface images, Fig. 4a, show a smooth surface with the presence of few pores. SEM cross-section images, Fig. 4b, show that the polymer microstructure of the produced membrane is characterized by interconnected spherical pores (pores inside the pores) with an average diameter of ≈60 µm. In Fig. 4c it is possible to observe the presence of the TiO_2 nanoparticles over the pore wall. EDX analysis (Fig. 4d) allowed to identify carbon (C) and fluorine (F), corresponding to PVDF-TrFE; while titanium (Ti) and oxygen (O) correspond to the TiO_2 nanoparticles. The elemental quantification is presented in supplementary material (Table A1). EDX mapping analysis also presented in Fig. 4d confirms the homogeneous distribution of TiO_2 nanoparticles over the membrane, indicated by the Ti signature (red dots over the image).

Furthermore, as reported in [37,46], the polymer crystallizes in the polar β-phase, and no chemical bonds between the polymer and the TiO_2 nanoparticles were identified. Additionally, the nanocomposites possess a porosity ranging from ≈70 to 80%.

3.2. Photocatalytic degradation of tartrazine

The photocatalytic activity of the 8% TiO_2/P(VDF–TrFE) membrane [37,40] was used in this work to assess the degradation of tartrazine. Fig. 5 shows the degradation profile of tartrazine ($10\,mg\,l^{-1}$) after 5 h (300 min) of sunlight irradiation indicating that approximately 78% of the dye was degraded, at a reaction rate constant of $0.30\,min^{-1}$.

As a control, the same experiment was carried out without the 8% TiO_2/P(VDF–TrFE) membrane and, under this condition, just 2% of degradation was observed after sunlight irradiation of the tartrazine solution for 5 h. This result shows that this dye is stable under sunlight irradiation, presenting low photolysis, which agrees with [47,48]. In the presence of the produced membrane but the absence of sunlight, 9% of tartrazine removal was observed after

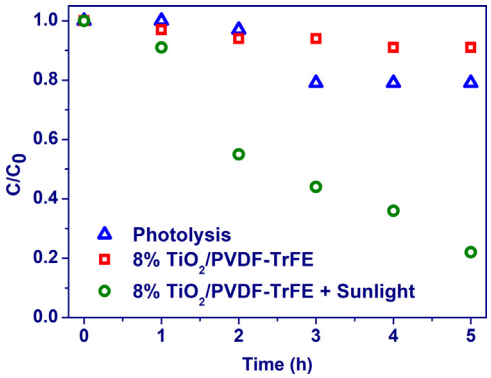

Fig. 5. Photocatalytic degradation of tartrazine (10 mg l^{-1}) with the 8 wt% TiO_2/PVDF–TrFE nanocomposite, over 5 h of sunlight irradiation. Controls: irradiation of tartrazine solution without the nanocomposite (photolysis); the nanocomposite in tartrazine solution with no irradiation (adsorption).

5 h (Fig. 5), which can be addressed to adsorption of dye into the 8 wt% TiO_2/PVDF-TrFE nanocomposite membrane.

As previously mentioned, few works have reported on tartrazine degradation in immobilized systems [42,49,50] using different approaches like the one presented in this work. Thus, given the different set-ups and experimental conditions of these works, is not possible to make a direct comparison of the results. The utmost similar work also using a solar photoreactor, was based on TiO_2 (P25) impregnated on the photoreactor surface to degrade tartrazine [49]. The results show that 99% of the dye was degraded after 5 h of sunlight radiation. The system mentioned above is based on particles fixed to the photoreactor surface, but the nanoparticles are not embedded into any substrate or matrix – reducing the surface area loss when compared to our system. Additionally, this work employs a significantly larger photoreactor (1 × 0.5 m), and the estimated amount of TiO_2 nanoparticles was almost 2-fold (1.8×) the amount used in our study. Furthermore, the impregnation of the nanocatalyst directly into the photoreactor surface will require a laborious process to clean and re-impregnate it with a new TiO_2 layer for eventual further reuse, a task that was not addressed. On the other hand, our system allows a simple and fast monitorization/substitution of the photocatalytic nanocomposite for the proper recycling of the remaining residues. TiO_2 nanoparticles have also been immobilized by sol-gel on calcinated sewage sludge and ≈80% of tartrazine was degraded under visible radiation (82 lm W^{-1}) for 120 min [50]. The drawback of this system is the same presented by slurry systems, which require sedimentation and decantation processes that are time-consuming and expensive.

Other works, where the UV lamps were used instead of sunlight radiation also serve as a reference but not for straightforward comparison; for instance, nanocomposites based on TiO_2 and activated carbon were able to degrade 80% of tartrazine in 3 h (UV – 4.7 mW/cm^2) [42]. The authors mentioned that the obtained efficiency is owed to the adsorptive properties of the activated carbon that transfers the adsorbed organic compounds to the active catalytic sites on the TiO_2 surface. Moreover, despite the promising results, this suspension system does not avoid the time-consuming and expensive recuperation processes, which is a hindrance concerning the reusability of photocatalytic materials.

3.3. Effect of initial dye concentration

The effect of initial tartrazine concentration on the photocatalytic activity was studied by degrading tartrazine solutions of 10, 20 and 30 mg l^{-1}. It was found that degradation percentage is strongly dependent on the initial dye concentration and decreased from ≈78 to 46% with increasing concentration of the dye, from 10 to 30 mg l^{-1} (Fig. 6).

Table 1
Effect of initial dye concentration (C_0) on photocatalytic degradation efficiency (%) and apparent reaction rate (K_{app}) of tartrazine.

C_0 (mg L^{-1})	Degradation (%)	K_{app} (min^{-1})	R^2
10	77.77	0.30	0.96
20	57.72	0.18	0.97
30	46.57	0.12	0.98

The rate of degradation is related to the available catalyst surface for the generation of electron-hole pairs, which in turn generates hydroxyl radicals. In this case, the amount of catalyst is kept constant, and the number of hydroxyl radicals generated remains the same, while dye concentration increases. Therefore, the ratio of *hydroxyl radical/tartrazine molecules* decreases with higher concentrations [50], leading to lower photodegradation efficiencies. Additionally, higher tartrazine concentrations will also reduce the UV light absorbance by TiO_2 nanoparticles surface, which will also contribute to decreasing the amount of hydroxyl radicals formed [44]. In this context, the photocatalytic efficiency reduces in high concentrated tartrazine solutions.

The kinetics of photocatalytic degradation of tartrazine can be described by the first-order equation (Eq. 2) [51].

$$ln\left(\frac{C_0}{C_t}\right) = K_{app}t \quad (2)$$

where K_{app} is the pseudo-first order rate constant (min^{-1}), C_o is the initial concentration, and C_t is the concentration of tartrazine at time t (min). Fig. 6b shows the plot of ln (C_t/C_0) *vs.* time at different initial dye concentrations. Linear plots were observed (with R^2 values higher than 0.9), which confirms that the photocatalytic degradation of tartrazine obeys a pseudo-first order kinetics. The estimated pseudo-first order rate constant and corresponding R^2 values are presented in Table 1. With increasing dye concentration from 10 to 30 mg/l, the degradation rate constant decreases from 0.30 to 0.12 min^{-1}. Other works reporting on at the effect of initial tartrazine concentration on the photocatalytic process also confirm a similar trend: higher initial concentrations yield lower degradation constants [49,52].

The Langmuir–Hinshelwood model has also been used to evaluate the heterogeneous photocatalytic reaction of organic compounds in aqueous solutions [53]. The experimental data were then represented concerning the Langmuir–Hinshelwood model to accommodate reactions taking place at the solid-liquid interface, (Eqs. (3) and (4)) [54].

$$r_0 = -\frac{dC}{dt} = \frac{K_1K_2C}{(1+K_2C_0)} = K_{app}C \quad (3)$$

$$\frac{1}{K_{app}} = \frac{1}{K_1K_2} + \frac{C_0}{K_1} \quad (4)$$

where r_o is the rate of degradation of the dye, K_1 is the surface reaction rate constant (mol l^{-1} min^{-1}), and K_2 is the Langmuir-Hinshelwood adsorption equilibrium constant (l mol^{-1}). The plot of $1/K_{app}$ *vs.* C_o for the photocatalytic degradation of tartrazine is shown in Fig. 7.

The linear relationship between $1/K_{app}$ and C_o (R^2 = 0.995) indicates the validity and applicability of the Langmuir – Hinshelwood model for photocatalytic degradation of tartrazine by the 8 wt% TiO_2/P(VDF–TrFE) membrane suggesting that tartrazine degradation occurs mostly on nanoparticles surface, in good agreement with other works [50]. The values of K_1 and K_2 were found to be 5.4 mol l^{-1} min^{-1} and 4 l mol^{-1}, respectively.

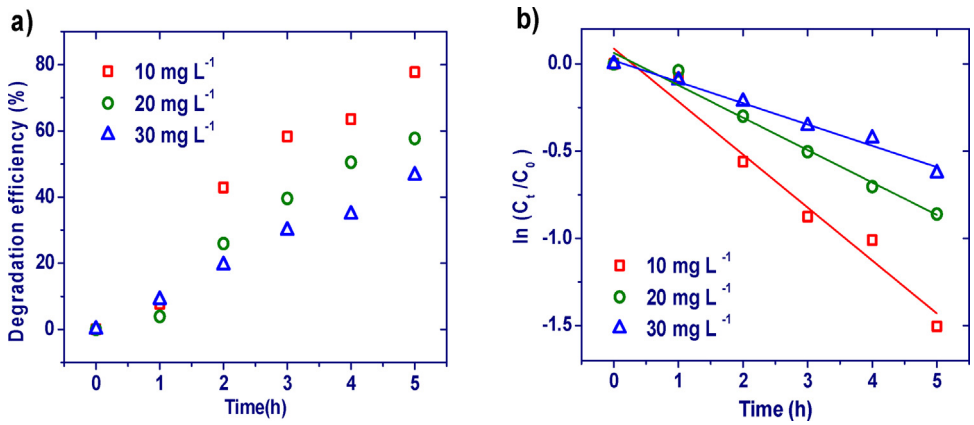

Fig. 6. Degradation efficiency (%) (a) and ln (C_t/C_0) *vs.* time (b) for different initial dye concentration (10, 20 and 30 mg^{l-1}), using 8 wt% TiO_2/PVDF-TrFE nanocomposites under sunlight irradiation over 5 h.

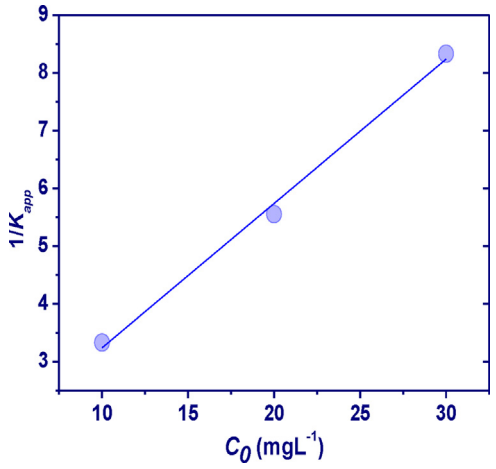

Fig. 7. Plot of $1/K_{app}$ as a function of the initial concentration (C_0) of tartrazine.

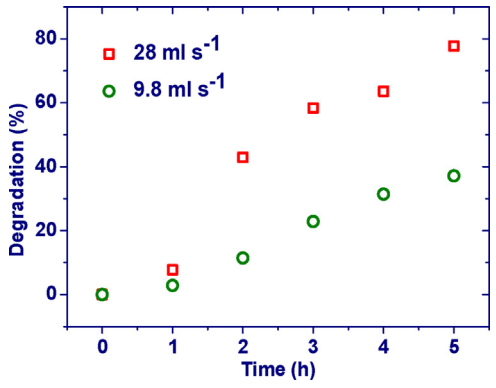

Fig. 8. Degradation of tartrazine ($C_0 = 10\ mgl^{-1}$) at different circulation flowrates with an 8%wt TiO_2/PVDF–TrFE nanocomposite and free pH (6.2) under 5 h of solar irradiation.

3.4. Effect of flow rate

The effect of tartrazine solution flow rate in the photocatalytic degradation was investigated by testing two different flow rates: 9.78 ml s^{-1} and 28 ml s^{-1}. Fig. 8 shows that the degradation of tartrazine increases almost linearly with time for both flow rates tested. After 5 h of UV irradiation, the percent degradation of tartrazine was 37% and 77% for 9.78 ml s^{-1} and 28 ml s^{-1}, respectively.

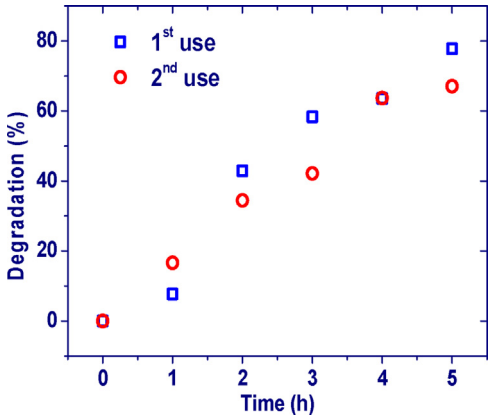

Fig. 9. Photocatalytic degradation of tartrazine ($C_0 = 10\ mgl^{-1}$) with an 8%wt TiO_2/PVDF–TrFE nanocomposite in two consecutive uses, under 5 h of sunlight exposure.

The increase in degradation efficiency at a higher flow rate is ascribed to a larger turbulence in the solution, which promotes the external mass transfer from the bulk solution to TiO_2/PVDF–TrFE nanocomposite surface. This conditions will indirectly increase the global rate of reaction between the TiO_2/PVDF–TrFE nanocomposite and tartrazine and in turn will result in higher percent degradation of tartrazine. In fact, Amid Amiri and co-workers also found that increasing the flow rate throughout membranes coated with zinc oxide nanoparticles promoted higher Reactive Yellow degradation rates, caused by enhanced mass transfer [55].

3.5. Reusability of the TiO_2/P(VDF-TrFE) nanocomposite membrane

The reusability of the nanocomposite was also assessed, and two uses were performed. Between the first and the second uses the nanocomposite membrane was rinsed with distilled water and dried at room temperature. Afterward, a new tartrazine solution was added to the photoreactor and a second use performed, under the same experimental conditions. The results presented in Fig. 9 show that ≈ 78% of tartrazine was degraded after 5 h of sunlight exposure. For a second use, ≈ 67% of tartrazine was degraded, which corresponds to ≈10% of efficiency loss. No further reuses were performed, as it has been demonstrated that most nanoparticles inefficiently attached to the polymer matrix detach during the first use and cleaning step [46,56,57].

This loss of photocatalytic efficiency is explained by the washing out of TiO_2 nanoparticles from the surface of the PVDF-TrFE mem-

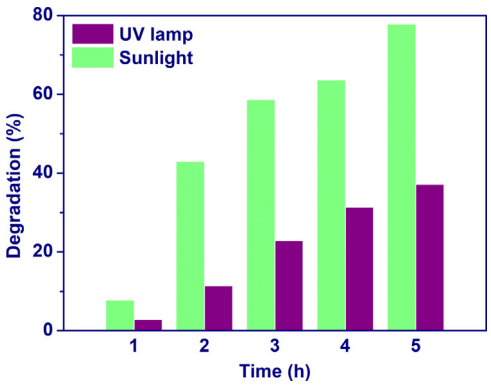

Fig. 10. Comparative degradation of tartrazine ($C_0 = 10\,mgl^{-1}$) with an 8%wt TiO_2/PVDF–TrFE nanocomposite under 5 h of solar or UV lamp irradiation.

brane, during the first use and posterior cleaning step. The second use corresponds to the photocatalytic process involving the TiO_2 nanoparticles more efficiently retained on the microporous structure, in good agreement with the SEM and EDX mapping Images – where high amounts of nanoparticles are distributed inside the pores. Previous reports on the recyclability of the nanocomposite indicate similar efficiencies losses (16% after 3 cycles) for a 10 wt% TiO_2 PVDF-TrFE nanocomposite used for methylene blue degradation [46]. This efficiency loss is in the order of the losses observed in related immobilization strategies. Thus, a TiO_2-RGO/nylon-6 nanocomposite produced by electrospinning and hydrothermal treatment revealed a slight photocatalytic efficiency loss (<10%) after 4 cycles of methylene blue degradation [58]; a sol-gel membrane containing TiO_2, silicon dioxide (SiO_2) and silicon carbide (SiC) was used to degrade methylene blue and for some of the produced membranes, the efficiency decreased 2.3, 3 and 5 times during the second use [59]; finally, pluronic-based TiO_2 hybrid photocatalytic membranes suffered a reduction of ≈9% after 5 cycles for Rhodamine B degradation [60]. In all these works, the efficiency loss was explained by the loss of nanoparticles from the substrate, which is one of the larger hurdles immobilized systems [21]. Additionally, the efficiency loss can also be related to the high amount of accumulated dye (after the consecutive uses) on the membrane surface and the consequent diminishing specific photo catalytically active sites [60]. Thus, considering the literature and the obtained results, the produced photocatalytic nanocomposites demonstrate a suitable reusability.

3.6. *Effect of irradiation intensity*

The influence of irradiation intensity on the degradation efficiency of the 8 wt% TiO2/PVDF-TrFE nanocomposite was assessed exposing the nanocomposite and tartrazine solution to a UV lamp or sunlight irradiation (Fig. 10).

As mentioned before, during 5 h of sunlight exposure, the 8%wt TiO_2/PVDF–TrFE nanocomposite placed on the photoreactor could degrade ≈78% of tartrazine. In comparison using a UV lamp, under the same experimental conditions, there was a significant photocatalytic efficiency decrease, and just ≈37% of tartrazine was degraded. These results indicate a remarkable photocatalytic activity under sunlight radiation, especially because TiO_2 requires UV radiation (<387 nm) to be photocatalytic active, which corresponds to only ≈5% of the radiation provided by the sun [61]. The different intensity of the UV lamp and UV from sunlight during the photocatalytic experiments, respectively 6 mW/cm^2 and 60–100 mW/cm^2 (Supplementary material Figure A1), explains the differences observed in the photocatalytic degradation. However, higher light intensities do not always guarantee higher photocatalytic efficiencies, and studies with different compounds have shown the nonlinear relationship between these two variables, due to the higher electron-hole recombination rate that may occur under high light intensities [51,53]. However, our results show that a significant increase in light intensity (≥10×) yielded an enhanced tartrazine degradation efficiency. These results are consistent with the results obtained by Salam K. Al-Dawery, which demonstrated the linear relationship between the light intensity and degradation rate and identified light intensity as the main factor in the tartrazine degradation kinetic [44]. The work developed by Chekir and coworkers also shows that tartrazine was more efficiently degraded by TiO_2 under solar radiation than with UV lamp radiation [49].

4. Conclusions

The degradation of persistent and hazardous organic chemicals such as tartrazine is urgent to avoid environmental impacts. In this work, a TiO_2/PVDF–TrFE nanocomposite membrane with an interconnected pores microstructure was produced and used for tartrazine photocatalytic degradation in a solar photoreactor. The nanocomposite displays an even distribution of the TiO_2 nanoparticles over the pore walls. Tartrazine solutions of 10, 20 and 30 mgl^{-1} presented degradation efficiencies of 78, 58 and 47% respectively, after 5 h of solar irradiation. The results show that the photocatalytic degradation of tartrazine obeys a pseudo-first-order kinetics and that degradation occurs mainly on nanoparticles surface. Decreasing the UV radiation intensity (UV lamp) reduces the photocatalytic degradation of tartrazine to 37%. Finally, a reusability assay was performed, and the nanocomposite proved to be effective, as the nanoparticles efficiently attached/retained in the polymeric porous structure allow for an efficient photocatalytic performance. These results indicate the feasibility of the scale-up process for the TiO_2/PVDF-TrFE nanocomposite and the suitability of this nanocomposite membrane for application in solar photoreactors for the degradation of tartrazine and related pollutants.

Acknowledgements

This work was supported by the Solar Equipment Development Unit (UDES) Algeria. This work was also supported by the Portuguese Foundation for Science and Technology (FCT) in the framework of the strategic project UID/FIS/04650/2013 by FEDER funds through the COMPETE 2020-Programa Operacional Competitividade e Internacionalização (POCI) with the reference project POCI-01-0145-FEDER-006941, and project PTDC/CTM-ENE/5387/2014. P.M. Martins thanks the FCT for the grant SFRH/ BD/ 98616/ 2013.The authors acknowledge funding from the Basque Government Industry Department under the ELKARTEK Program and the Spanish Ministry of Economy and Competitiveness (MINECO) through the project MAT2016-76039-C4-3-R (AEI/FEDER, UE) (including the FEDER financial support).

Appendix A. Supplementary data

Supplementary data associated with this article can be found, in the online version, at https://doi.org/10.1016/j.jhazmat.2017.10.053.

References

[1] M.A. Shannon, P.W. Bohn, M. Elimelech, J.G. Georgiadis, B.J. Marinas, A.M. Mayes, Science and technology for water purification in the coming decades, Nature 452 (2008) 301–310.
[2] X. Ke, S. Ribbens, Y. Fan, H. Liu, P. Cool, D. Yang, H. Zhu, Integrating efficient filtration and visible-light photocatalysis by loading Ag-doped zeolite Y particles on filtration membrane of alumina nanofibers, J. Membr. Sci. 375 (2011) 69–74.

[3] M.J. Iqbal, M.N. Ashiq, Adsorption of dyes from aqueous solutions on activated charcoal, J. Hazard. Mater. 139 (2007) 57–66.
[4] D. Bilba, D. Suteu, T. Malutan, Removal of reactive dye brilliant red HE-3 B from aqueous solutions by hydrolyzed polyacrylonitrile fibres: equilibrium and kinetics modelling, Cent. Eur. J. Chem. 6 (2008) 258.
[5] P.K. Gautam, R.K. Gautam, S. Banerjee, G. Lofrano, M.A. Sanroman, M.C. Chattopadhyaya, J.D. Pandey, Preparation of activated carbon from Alligator weed (Alternenthera philoxeroids) and its application for tartrazine removal: isotherm, kinetics and spectroscopic analysis, J. Environ. Chem. Eng. 3 (2015) 2560–2568.
[6] U. Pagga, D. Brown, The degradation of dyestuffs: part II behaviour of dyestuffs in aerobic biodegradation tests, Chemosphere 15 (1986) 479–491.
[7] J.-H. Sun, S.-P. Sun, G.-L. Wang, L.-P. Qiao, Degradation of azo dye amido black 10 B in aqueous solution by fenton oxidation process, Dyes Pigm. 74 (2007) 647–652.
[8] B.H. Hameed, Evaluation of papaya seeds as a novel non-conventional low-cost adsorbent for removal of methylene blue, J. Hazard. Mater. 162 (2009) 939–944.
[9] T. Tanaka, Reproductive and neurobehavioural toxicity study of tartrazine administered to mice in the diet, Food Chem. Toxicol. 44 (2006) 179–187.
[10] I. Moutinho, L. Bertges, R. Assis, Prolonged use of the food dye tartrazine (FD&C yellow n° 5) and its effects on the gastric mucosa of Wistar rats, Braz. J. Biol. 67 (2007) 141–145.
[11] B.M. Soares, T.M.T. Araújo, J.A.B. Ramos, L.C. Pinto, B.M. Khayat, M. De Oliveira Bahia, R.C. Montenegro, R.M.R.G. Burbano, A.S. Khayat, Effects on DNA repair in human lymphocytes exposed to the food dye tartrazine yellow, Anticancer Res. 35 (2015) 1465–1474.
[12] L. Khayyat, A. Essawy, J. Sorour, A. Soffar, Tartrazine induces structural and functional aberrations and genotoxic effects in vivo, PeerJ 5 (2017) e3041.
[13] N.K. Tripathy, K.K. Patnaik, M.J. Nabi, Genotoxicity of tartrazine studied in two somatic assays of Drosophila melanogaster, Mutat. Res./Genet. Toxicol. 224 (1989) 479–483.
[14] M.P. Merville, J. Decuyper, M. Lopez, J. Piette, A. Van De Vorst, Phototoxic potentialities of tartrazine: screening tests, Photochem. Photobiol. 40 (1984) 221–226.
[15] V.K. Gupta, R. Jain, A. Nayak, S. Agarwal, M. Shrivastava, Removal of the hazardous dye—Tartrazine by photodegradation on titanium dioxide surface, Mater. Sci. Eng. C 31 (2011) 1062–1067.
[16] M.N. Chong, B. Jin, C.W.K. Chow, C. Saint, Recent developments in photocatalytic water treatment technology: a review, Water Res. 44 (2010) 2997–3027.
[17] S. Ahmed, M.G. Rasul, W.N. Martens, R. Brown, M.A. Hashib, Heterogeneous photocatalytic degradation of phenols in wastewater: a review on current status and developments, Desalination 261 (2010) 3–18.
[18] R. Vinu, G. Madras, Kinetics of sonophotocatalytic degradation of anionic dyes with nano-TiO2, Environ. Sci. Technol. 43 (2009) 473–479.
[19] R. Scotti, M. D'Arienzo, F. Morazzoni, I.R. Bellobono, Immobilization of hydrothermally produced TiO2 with different phase composition for photocatalytic degradation of phenol, Appl. Catal. B Environ. 88 (2009) 323–330.
[20] R.L. Pozzo, M.A. Baltanás, A.E. Cassano, Supported titanium oxide as photocatalyst in water decontamination: state of the art, Catal. Today 39 (1997) 219–231.
[21] A.Y. Shan, T.I.M. Ghazi, S.A. Rashid, Immobilisation of titanium dioxide onto supporting materials in heterogeneous photocatalysis: a review, Appl. Catal. A Gen. 389 (2010) 1–8.
[22] M.M. Momeni, Y. Ghayeb, S. Gheibee, Silver nanoparticles decorated titanium dioxide-tungsten trioxide nanotube films with enhanced visible light photo catalytic activity, Ceram. Int. 43 (2017) 564–570.
[23] M.M. Momeni, Y. Ghayeb, Photochemical deposition of platinum on titanium dioxide-tungsten trioxide nanocomposites: an efficient photocatalyst under visible light irradiation, J. Mater. Sci.: Mater. Electron. 27 (2016) 1062–1069.
[24] N.A. Almeida, P.M. Martins, S. Teixeira, J.A. Lopes da Silva, V. Sencadas, K. Kühn, G. Cuniberti, S. Lanceros-Mendez, P.A.A.P. Marques, TiO_2/graphene oxide immobilized in P(VDF-TrFE) electrospun membranes with enhanced visible-light-induced photocatalytic performance, J. Mater. Sci. 51 (2016) 6974–6986.
[25] M.M. Momeni, Y. Ghayeb, A.A. Mozafari, Optical and photo catalytic characteristics of Ag2S/TiO2 nanocomposite films prepared by electrochemical anodizing and SILAR approach, J. Mater. Sci. 27 (2016) 11201–11210.
[26] M.M. Momeni, Z. Nazari, Preparation of TiO2 and WO3-TiO2 nanotubes decorated with PbO nanoparticles by chemical bath deposition process: a stable and efficient photo catalyst, Ceram. Int. 42 (2016) 8691–8697.
[27] M.M. Momeni, Y. Ghayeb, Preparation of cobalt coated TiO2 and WO3-TiO2 nanotube films via photo-assisted deposition with enhanced photocatalytic activity under visible light illumination, Ceram. Int. 42 (2016) 7014–7022.
[28] A. Alem, H. Sarpoolaky, M. Keshmiri, Sol-gel preparation of titania multilayer membrane for photocatalytic applications, Ceram. Int. 35 (2009) 1837–1843.
[29] S. Mozia, Photocatalytic membrane reactors (PMRs) in water and wastewater treatment. A review, Sep. Purif. Technol. 73 (2010) 71–91.
[30] S.S. Chin, K. Chiang, A.G. Fane, The stability of polymeric membranes in a TiO_2 photocatalysis process, J. Membr. Sci. 275 (2006) 202–211.
[31] M.E. Fabiyi, R.L. Skelton, Photocatalytic mineralisation of methylene blue using buoyant TiO2-coated polystyrene beads, J. Photochem. Photobiol. A 132 (2000) 121–128.
[32] K. Tennakone, C.T.K. Tilakaratne, I.R.M. Kottegoda, Photocatalytic degradation of organic contaminants in water with TiO2 supported on polythene films, J. Photochem. Photobiol. A 87 (1995) 177–179.
[33] E. Cossich, R. Bergamasco, M.T. Pessoa de Amorim, P.M. Martins, J. Marques, C.J. Tavares, S. Lanceros-Méndez, V. Sencadas, Development of electrospun photocatalytic TiO_2-polyamide-12 nanocomposites, Mater. Chem. Phys. 164 (2015) 91–97.
[34] R.A. Damodar, S.-J. You, H.-H. Chou, Study the self cleaning, antibacterial and photocatalytic properties of TiO_2 entrapped PVDF membranes, J. Hazard. Mater. 172 (2009) 1321–1328.
[35] J. Nunes-Pereira, C.M. Costa, R.E. Sousa, A.V. Machado, M.M. Silva, S. Lanceros-Méndez, Li-ion battery separator membranes based on barium titanate and poly(vinylidene fluoride-co-trifluoroethylene): filler size and concentration effects, Electrochim. Acta 117 (2014) 276–284.
[36] A. Ferreira, J. Silva, V. Sencadas, J.L.G. Ribelles, S. Lanceros-Méndez, Poly[(vinylidene fluoride)-co-trifluoroethylene] membranes obtained by isothermal crystallization from solution, Macromol. Mater. Eng. 295 (2010) 523–528.
[37] P.M. Martins, R. Miranda, J. Marques, C.J. Tavares, G. Botelho, S. Lanceros-Mendez, Comparative efficiency of TiO_2 nanoparticles in suspension vs. immobilization into P(VDF-TrFE) porous membranes, RSC Adv. 6 (2016) 12708–12716.
[38] G. Botelho, M.M. Silva, A.M. Gonçalves, V. Sencadas, J. Serrado-Nunes, S. Lanceros-Mendez, Performance of electroactive poly(vinylidene fluoride) against UV radiation, Polym. Test. 27 (2008) 818–822.
[39] P. Martins, A.C. Lopes, S. Lanceros-Mendez, Electroactive phases of poly(vinylidene fluoride): Determination, processing and applications, Prog. Polym. Sci. 39 (2014) 683–706.
[40] P.M. Martins, V. Gomez, A.C. Lopes, C.J. Tavares, G. Botelho, S. Irusta, S. Lanceros-Mendez, Improving photocatalytic performance and recyclability by development of er-doped and Er/Pr-codoped TiO_2/poly(vinylidene difluoride)-trifluoroethylene composite membranes, J. Phys. Chem. C 118 (2014) 27944–27953.
[41] K.V.S. Rao, B. Lavédrine, P. Boule, Influence of metallic species on TiO2 for the photocatalytic degradation of dyes and dye intermediates, J. Photochem. Photobiol. A 154 (2003) 189–193.
[42] C. Andriantsiferana, E.F. Mohamed, H. Delmas, Photocatalytic degradation of an azo-dye on TiO2/activated carbon composite material, Environ. Technol. 35 (2014) 355–363.
[43] V. Vaiano, G. Iervolino, D. Sannino, L. Rizzo, G. Sarno, P. Ciambelli, L.A. Isupova, Food azo-dyes removal from water by heterogeneous photo-Fenton with LaFeO3 supported on honeycomb corundum monoliths, J. Environ. Eng. 141 (2015) 04015038.
[44] S.K. Al-Dawery, Enhanced dynamics characterization of photocatalytic decolorization of hazardous dye tartrazine using titanium dioxide, Desalin. Water Treat. 57 (2016) 8851–8859.
[45] R.Y. Hong, J.H. Li, L.L. Chen, D.Q. Liu, H.Z. Li, Y. Zheng, J. Ding, Synthesis, surface modification and photocatalytic property of ZnO nanoparticles, Powder Technol. 189 (2009) 426–432.
[46] S. Teixeira, P.M. Martins, S. Lanceros-Méndez, K. Kühn, G. Cuniberti, Reusability of photocatalytic TiO_2 and ZnO nanoparticles immobilized in poly(vinylidene difluoride)-co-trifluoroethylene, Appl. Surf. Sci. 384 (2016) 497–504.
[47] T.C. dos Santos, G.J. Zocolo, D.A. Morales, G.d.A. Umbuzeiro, M.V.B. Zanoni, Assessment of the breakdown products of solar/UV induced photolytic degradation of food dye tartrazine, Food Chem. Toxicol. 68 (2014) 307–315.
[48] K. Tanaka, K. Padermpole, T. Hisanaga, Photocatalytic degradation of commercial azo dyes, Water Res. 34 (2000) 327–333.
[49] N. Chekir, D. Tassalit, O. Benhabiles, N. Kasbadji Merzouk, M. Ghenna, A. Abdessemed, R. Issaadi, A comparative study of tartrazine degradation using UV and solar fixed bed reactors, Int. J. Hydrogen Energy 42 (2017) 8948–8954.
[50] T.S. Jamil, S.E.A. Sharaf El-Deen, Removal of persistent tartrazine dye by photodegradation on TiO_2 nanoparticles enhanced by immobilized calcinated sewage sludge under visible light, Sep. Sci. Technol. 51 (2016) 1744–1756.
[51] S. Ahmed, M.G. Rasul, R. Brown, M.A. Hashib, Influence of parameters on the heterogeneous photocatalytic degradation of pesticides and phenolic contaminants in wastewater: a short review, J. Environ. Manage. 92 (2011) 311–330.
[52] C.L. Heredia, d.L. Sham, l.M. Farfán-Torres, Tartrazine degradation by supported TiO_2 on magnetic particles, Matéria (Rio de Janeiro) 20 (2015) 668–675.
[53] M.R. Hoffmann, S.T. Martin, W. Choi, D.W. Bahnemann, Environmental applications of semiconductor photocatalysis, Chem. Rev. 95 (1995) 69–96.
[54] L.-Y. Yang, S.-Y. Dong, J.-H. Sun, J.-L. Feng, Q.-H. Wu, S.-P. Sun, Microwave-assisted preparation, characterization and photocatalytic properties of a dumbbell-shaped ZnO photocatalyst, J. Hazard. Mater. 179 (2010) 438–443.
[55] H. Amiri, B. Ayati, H. Ganjidoust, Mass transfer phenomenon in photocatalytic cascade disc reactor: effects of artificial roughness and flow rate, Chem. Eng. Process. Process Intensif. 116 (2017) 48–59.
[56] A. Snyder, Z. Bo, R. Moon, J.-C. Rochet, L. Stanciu, Reusable photocatalytic titanium dioxide-cellulose nanofiber films, J. Colloid Interface Sci. 399 (2013) 92–98.
[57] T. Harifi, M. Montazer, A novel magnetic reusable nanocomposite with enhanced photocatalytic activities for dye degradation, Sep. Purif. Technol. 134 (2014) 210–219.

[58] H.R. Pant, B. Pant, P. Pokharel, H.J. Kim, L.D. Tijing, C.H. Park, D.S. Lee, H.Y. Kim, C.S. Kim, Photocatalytic TiO_2-RGO/nylon-6 spider-wave-like nano-nets via electrospinning and hydrothermal treatment, J. Membr. Sci. 429 (2013) 225–234.
[59] R.M. Huertas, M.C. Fraga, J.G. Crespo, V.J. Pereira, Sol-gel membrane modification for enhanced photocatalytic activity, Sep. Purif. Technol. 180 (2017) 69–81.
[60] R. Goei, Z. Dong, T.-T. Lim, High-permeability pluronic-based TiO_2 hybrid photocatalytic membrane with hierarchical porosity: fabrication, characterizations and performances, Chem. Eng. J. 228 (2013) 1030–1039.
[61] Y.Y. Gurkan, E. Kasapbasi, Z. Cinar, Enhanced solar photocatalytic activity of TiO_2 by selenium(IV) ion-doping: characterization and DFT modeling of the surface, Chem. Eng. J. 214 (2013) 34–44.